ChemComm

ROYAL SOCIETY OF CHEMISTRY

COMMUNICATION

View Article Online
View Journal | View Issue

Check for updates

Cite this: *Chem. Commun.*, 2025, **61**, 2822

Received 27th November 2024,
Accepted 16th January 2025

DOI: 10.1039/d4cc06293k

rsc.li/chemcomm

Synthesis of fully fused tetrapyrazinoporphyrazine polymers bearing three-dimensional structures controlled by steric repulsion†

Kosuke Watanabe,[ab] Teruki Toya,[c] Yuto Toyota,[c] Yoichi Kobayashi,[c] Junichi Usuba,[d] Yuh Hijikata,[d] Ryotaro Matsuda,[de] Katsuyuki Nishimura,[ab] Haruki Sugiyama[abf] and Yasutomo Segawa *[ab]

The synthesis and characterization of fused aromatic networks composed of zinc tetrapyrazinoporphyrazines are reported. The steric repulsion of bulky substituents induced the formation of three-dimensional structures. Thus-obtained insoluble polymers adsorbed CO_2 and had near-infrared absorption indicating their porosity and extended π-conjugation.

Fused aromatic networks (FANs), the network polymers consisting of fully fused aromatic rings, have been intensively studied due to their unique structural, optical, and electronic properties.[1] While many types of two-dimensional (2D) FANs have been reported, 3D FANs have not been well studied due to the difficulty of constructing 3D networks with fused aromatic structures. To date, several examples of 3D FANs have been synthesized using nonplanar conjugated units and their structural features, thermal stability, porosity, and semiconductor properties have been studied. The 3D FANs with saddle-shaped cyclooctatetraene derivatives as nonplanar conjugated units exhibited physical and chemical stability, permanent porosity, high surface area, and semiconductor properties.[2] Triptycenes were also used as nonplanar conjugated units to form 3D FANs that exhibited high gas adsorption properties and thermal stability.[3]

Considering the high stability and electronic properties, phthalocyanines and their analogues are useful π-conjugated units. Phthalocyanine-based polymers have been studied for many years.[4] Based on band structure calculations, 1D and 2D fully fused polymers were predicted to exhibit electrical conductivity.[5] The synthesis of 2D phthalocyanine polymers was carried out both on metal surfaces and in solution.[6] However, only a few examples of 3D polymers have been reported. The 3D frameworks containing phthalocyanines reported so far were not conjugated because they were linked by sp^3 carbon or boron atoms.[7] An electrically neutral, spiro-linked phthalocyanine-containing 3D polymer was synthesized by McKeown and co-workers in 2004.[8] Later in 2017, Kimura and co-workers reported the synthesis of a spiro-conjugated 3D polymer using spirobifluorenes.[9]

To synthesize 3D FANs containing phthalocyanine analogues, we devised a strategy of using tetrapyrazinoporphyrazine (TPyzPz) and bending it with bulky substituents. TPyzPz is an analogue in which the benzene rings of phthalocyanine are replaced with pyrazine rings, and 2D FANs based on TPyzPz units have been synthesized (Fig. 1a).[10] Since the introduction of bulky substituents distorts phthalocyanines to be saddle-shaped structures,[11] we assumed that 2D and 3D FANs can be synthesized from tetracyanodihydrodipyrazinopyrazines (TCDP) depending on the size of the substituents (Fig. 1b). Herein, we report the synthesis of Zn TPyzPz FANs bearing 1-ethylpropyl and 2,4,6-trimethylphenyl (mesityl) groups. The crystallinity of the obtained solids was investigated by X-ray diffraction and the progress of the polymerization reaction was confirmed by using Fourier transform infrared (FT-IR) spectroscopy, solid-state ^{13}C nuclear magnetic resonance (NMR) spectroscopy, and diffuse reflectance spectroscopy. The thermal stability and porosity of the polymers were also measured by Thermogravimetric analysis (TG) measurements and adsorption–desorption experiments, respectively.

---

[a] *Institute for Molecular Science, Myodaiji, Okazaki, 444-8787, Japan. E-mail: segawa@ims.ac.jp*
[b] *The Graduate University for Advanced Studies, SOKENDAI, Myodaiji, Okazaki, 444-8787, Japan*
[c] *Department of Applied Chemistry, College of Life Sciences, Ritsumeikan University, 1-1-1 Nojihigashi, Kusatsu, Shiga 525-8577, Japan*
[d] *Research Center for Net Zero Carbon Society, Institute of Innovation for Future Society, Nagoya university, Nagoya, 464-8601, Japan*
[e] *Department of Chemistry and Biotechnology, School of Engineering, and Department of Materials Chemistry, Graduate School of Engineering, Nagoya University, Chikusa-ku, Nagoya, 464-8603, Japan*
[f] *Neutron Industrial Application Promotion Center, Comprehensive Research Organization for Science and Society, Tokai, Ibaraki 319-1106, Japan*

† Electronic supplementary information (ESI) available. CCDC 2403177–2403179 and 2404808. For ESI and crystallographic data in CIF or other electronic format see DOI: **https://doi.org/10.1039/d4cc06293k**

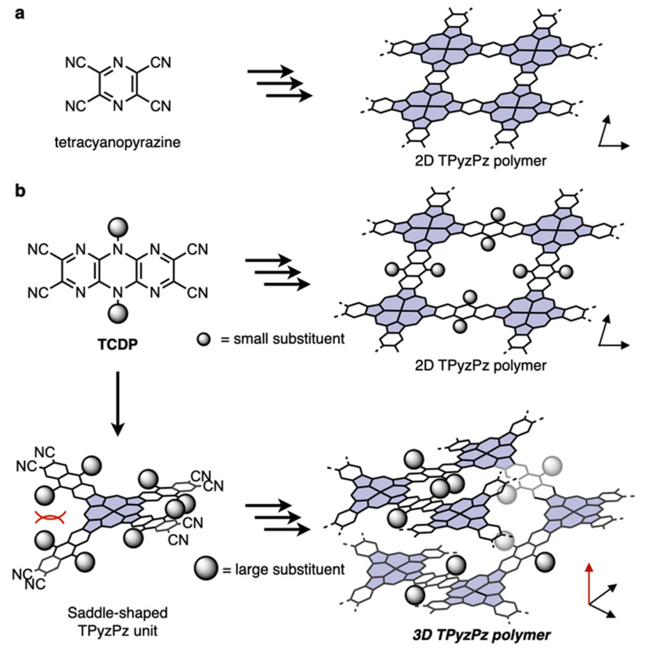

Fig. 1 (a) Previously reported 2D FANs based on TPyzPz units. (b) Synthetic strategy for 3D TPyzPz.

First, the structures of Zn TPyzPz dimers were optimized by density functional theory (DFT) calculations to investigate the influence of the substituent size on polymer networks. For the calculation, B3LYP method was used and LANL2DZ and 6-31G(d) basis sets were applied for Zn and other atoms, respectively (Fig. 2a). As shown in Fig. 2b, the dimer having 1-ethylpropyl groups (**DiEtPr**) adopts a planar structure. On the other hand, the optimized structures of the dimers having mesityl and 3,5-di-*t*-butylphenyl groups (**DiMes** and **DiBuPh**) are nonplanar in which the TPyzPz are distorted to be saddle-shaped structures. The bent angles of **DiMes** and **DiBuPh** are 145.3° and 123.3°, respectively, indicating that the bent angles increase with the substituent size caused by the steric repulsion of substituents. The dimer structure of **DiMes** was then extended to a 3D periodic structure and structural relaxation was performed by Quantum Espresso to obtain the framework structure with **dia-f** topology (see Fig. S1 for details, ESI†).[12] These calculations indicate that the TPyzPz polymers with bulky substituents hinder the formation of 2D sheet and result in a 3D network structure.

Monomers **3a–c** were prepared according to reported procedures with modifications (Fig. 3a).[13] The S_NAr reactions of dichlorodicyanopyrazine **1** with corresponding alkyl- and arylamines were carried out to produce monoaminated products **2a–c**. Dimerization of **2a–c** using triethylamine was performed in refluxing *N*,*N*-dimethylformamide (DMF) to obtain desired monomers **3a–c**. The monomers **3a–c** were identified by ^1H and ^{13}C NMR spectroscopy, mass spectrometry, and X-ray crystallography (see ESI† for details).

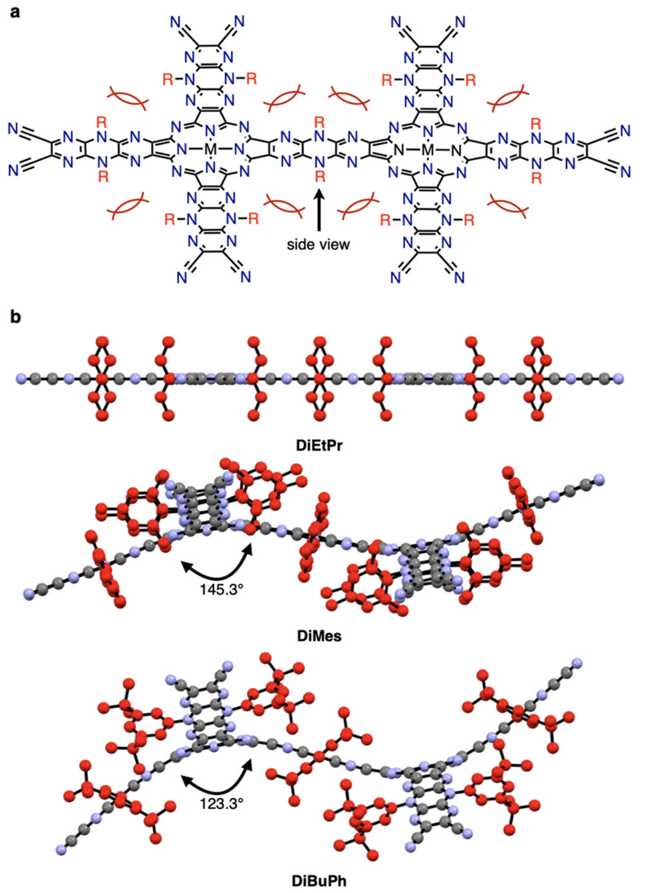

Fig. 2 (a) Structure of Zn TPyzPz dimer. (b) Optimized structures of **DiEtPr**, **DiMes**, and **DiBuPh**.

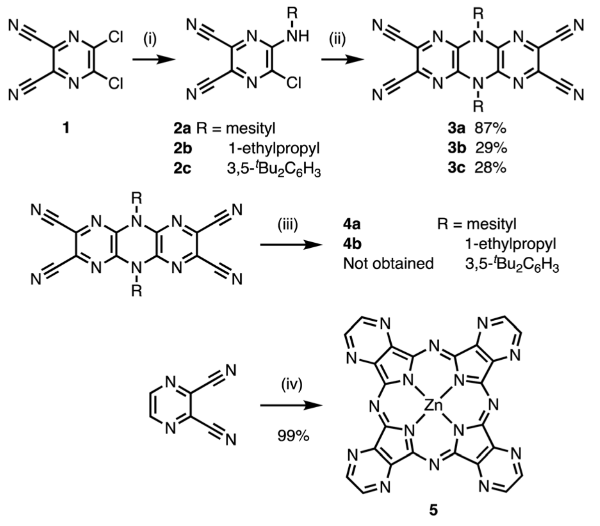

Fig. 3 Synthesis of **4a**, **4b**, and **5**. Reaction conditions: (i) RNH_2, THF, 0 °C to r.t., 6 h; (ii) NEt_3, DMF, reflux, 10 h; (iii) $ZnCl_2$, *n*-pentanol, NEt_3, DMAc, 100–200 °C, 10 days; (iv) $ZnCl_2$, *n*-pentanol, NEt_3, DMAc, 140 °C, 24 h.

With three monomers in hand, we investigated the polymerization reactions. As shown in Fig. 3, polymer **4a** was synthesized by the cyclotetramerization of the dicyanopyrazine moieties of monomer **3a** in the presence of anhydrous zinc chloride (0.5 equiv.), *n*-pentanol, and a catalytic amount of triethylamine in *N*,*N*-dimethylacetamide (DMAc).[10] The mixture was heated without stirring and the solution turned dark green as the reaction progressed. Polymer **4a** was obtained as an insoluble black solid and thoroughly washed with organic solvents and water. The use of diphenyl ether instead of DMAc as solvent afforded a brittle solid. In the reaction conditions using 1,8-diazabicyclo[5.4.0]-7-undecene as a base, no insoluble solid product was obtained. The optimized procedure using DMAc and triethylamine was also applied to **3b** and **3c**, and as a result, an insoluble black solid (polymer **4b**) was obtained from **3b** whereas no solid was formed from **3c**. These results indicate that **3a** and **3b** were polymerized to form highly crosslinked polymers. As described in Fig. 2b, the oligomers of **3a** cannot form a planar 2D sheet, suggesting the formation of 3D structures. On the other hand, no polymer was obtained from **3c**. Considering that the electronic effects of the mesityl and 3,5-di-*tert*-butylphenyl groups are comparable, the size of the substituent causes a significant difference in the reactivity of polymerization. The formation of TPyzPz structure was confirmed by the cyclotetramerization of 2,3-dicyanopyrazine under the reaction conditions using zinc chloride, *n*-pentanol and triethylamine in DMAc to obtain compound **5** in 99% isolated yield (Fig. 3).

To confirm the polymer structures in detail, a series of analyses were performed including FT-IR spectroscopy, solid-state ^{13}C NMR spectroscopy, energy dispersive spectroscopy (EDS), and powder X-ray diffraction (PXRD) measurement. FT-IR measurements of **4a**, **4b** and their monomers (**3a**, **3b**) were performed in air using an attenuated total reflectance method. Because the C$\equiv$N stretching peak at about 2230 cm^{-1} observed in the FT-IR spectra of monomers **3a** and **3b** disappeared in those of polymers **4a** and **4b**, it is inferred that the cyano groups were consumed (Fig. 4a). Solid-state ^{13}C NMR spectra of **4a** and **4b** using the cross polarization magic angle spinning with total suppression of sidebands (CP-MAS TOSS) method are shown in Fig. S9 and S10 (ESI†), respectively. In the spectrum of **4a**, aliphatic and aromatic signals derived from mesityl groups and TPyzPz moieties were observed. Signals attributed to DMAc were also observed at 160–170 ppm and 25–40 ppm. The spectrum of **4b** shows the signals corresponding to 1-ethylpropyl, TPyzPz, and DMAc. For **4b**, a small signal at 115 ppm was observed, which could be unreacted cyano groups. The EDS of **4a** and **4b** were performed using a Schottky emission scanning electron microscope. As shown in Fig. S11 and S12 (ESI†), C, N, and Zn elements are distributed throughout the surface of the solids. PXRD results of **4a** and **4b** supported the formation of partially ordered polymers (see ESI† for details).

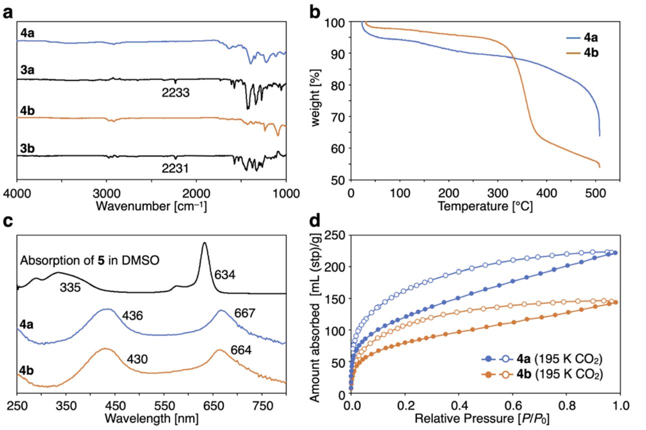

Fig. 4 (a) IR spectra of **3a**, **3b**, **4a**, and **4b**. (b) TG curves of **4a** and **4b**. (c) Diffuse reflectance spectra of **4a** and **4b**, and absorption spectrum of **5** in DMSO. (d) Adsorption isotherms of **4a** and **4b**.

TG was performed to investigate the thermal stability of polymers **4a** and **4b**. Before the measurement, polymers were soaked in diethyl ether and dried under vacuum. The weight loss derived from decomposition of **4b** was observed at around 300 °C, whereas no decomposition of **4a** was observed up to 500 °C (Fig. 4b). These differences in thermal stability are probably due to the 2D and 3D network structures.

In order to gain insight into the photophysical properties of **4a** and **4b**, diffuse reflectance spectroscopies were carried out. Each polymer was dispersed to 1 w% in magnesium oxide as dispersant and ground for 30 min prior to the measurements. The diffuse reflectance spectra of **4a** and **4b** are shown in Fig. 4c with the absorption spectrum of **5** in dimethyl sulfoxide (DMSO) solution as a reference. Both spectra show two broad peaks that can be assigned as Soret bands (**4a**: 436 nm, **4b**: 430 nm) and Q bands (**4a**: 667 nm, **4b**: 664 nm). In comparison to the absorption spectrum of **5** (soret: 335 nm, Q: 634 nm) in DMSO, the Soret and Q bands of **4a** were red-shifted by 101 and 33 nm (6.91×10^3 and 7.80×10^2 cm^{-1}), respectively, indicating the extension of π-conjugation through polymerization. Similar results were observed for **4b** (6.59×10^3 cm^{-1} for soret band and 7.13×10^2 cm^{-1} for Q band).

Adsorption–desorption experiments were carried out to investigate the porous properties of **4a** and **4b**. As shown in Fig. 4d, **4a** and **4b** showed adsorption behavior for CO_2. These results show the porous properties of **4a** and **4b**. The BET surface and Langmuir surface area of **4a** calculated from CO_2 adsorption are 581 and 576 m^2 g^{-1}, respectively, are slightly larger than those of **4b** (386 and 446 m^2 g^{-1}).

In summary, we have synthesized fused aromatic network polymers **4a** and **4b** and investigated their optical properties and porosity. Monomers **3a–3c** were prepared from dichlorodicyanopyrazine and aryl- or alkylamines in two steps. Polymerization of monomers **3a** and **3b** afforded insoluble black solids **4a** and **4b**, while no solid was obtained from **3c** indicating that 3,5-di-*tert*-butylphenyl groups were too bulky to polymerize. The consumption of cyano groups and the formation of Zn TPyzPz moieties were confirmed by IR spectra and solid-state ^{13}C NMR spectra. The formation of partially ordered polymers was supported by PXRD measurements. Differences in thermal stability, possibly due to the 2D and 3D network structures, were observed in TG-DTA measurements. The extension of π-conjugation through polymerization and the porous properties of the **4a** and **4b** were confirmed by diffuse reflectance spectroscopies and adsorption–desorption measurements, respectively. This work demonstrated the novel strategy for the synthesis of 3D FANs to create optically unique and porous organic materials.

This work was supported by FOREST program (JPMJFR211R to Y. S.) from JST, JSPS KAKENHI (JP22K19038 and JP22H02068 to Y. S.), Tatematsu Foundation and Murata Science and Education Foundation. We thank Prof. Yasuhiro Uozumi, Dr Taketoshi Minato, Ms Aya Tazawa (Institute for Molecular Science (IMS)), Dr Hirotoshi Sakamoto (Kyoto University) and Dr Masato Taki (Nagoya Institute of Technology) for their support of experiments and fruitful advices. K. W. is a recipient of JSPS Research Fellowship for Young Scientists (DC1). This work was conducted in IMS supported by ''Advanced Research Infrastructure for Materials and Nanotechnology in Japan (ARIM)'' of the Ministry of Education, Culture, Sports, Science and Technology (MEXT) (JPMXP1224MS5001, JPMXP1223 MS5011). Calculations were performed using the resources of the Research Center for Computational Science, Okazaki, Japan (24-IMS-C232). The solid-state NMR spectroscopy was supported by the Equipment Sharing Division, Organization for Co-Creation Research and Social Contributions, Nagoya Institute of Technology.

Data availability

Crystallographic data have been deposited at the CCDC under 2403177 (**3a**), 2403178 (**3b**), 2403179 (**3c**) and 2404808 (**5**). The data supporting this article have been included as the ESI† (pdf) and CartesianCoordinates.xyz (xyz) files.

Conflicts of interest

There are no conflicts to declare.

Notes and references

1 (*a*) S. Che and L. Fang, *Chem*, 2020, **6**, 2558–2590; (*b*) J. Mahmood, M. A. R. Anjum and J. B. Baek, *Adv. Mater.*, 2018, **31**, 1805062; (*c*) I. Ahmad, J. Mahmood and J. B. Baek, *Small Sci.*, 2021, **1**, 2000007.

2 (*a*) S. N. Talapaneni, J. Kim, S. H. Je, O. Buyukcakir, J. Oh and A. Coskun, *J. Mater. Chem. A*, 2017, **5**, 12080–12085; (*b*) Y. Byun, L. S. Xie, P. Fritz, T. Ashirov, M. Dinca and A. Coskun, *Angew. Chem., Int. Ed.*, 2020, **59**, 15166–15170; (*c*) T. Ashirov, P. W. Fritz, Y. Lauber, C. E. Avalos and A. Coskun, *Chem. – Eur. J.*, 2023, **29**, e202301053.

3 J. Mahmood, S. J. Kim, H. J. Noh, S. M. Jung, I. Ahmad, F. Li, J. M. Seo and J. B. Baek, *Angew. Chem., Int. Ed.*, 2018, **57**, 3415–3420.

4 N. B. McKeown, *J. Mater. Chem.*, 2000, **10**, 1979–1995.

5 P. Gomez-Romero, Y. S. Lee and M. Kertesz, *Inorg. Chem.*, 2002, **27**, 3672–3675.

6 (*a*) E. Nardi, M. Koudia, S. Kezilebieke, J.-P. Bucher and M. Abel, in On-surface synthesis, ed. A. Gourdon, *On-Surface Synthesis of Phthalocyanine Compounds*, Springer, Cham, 2016, pp. 115–129; (*b*) K. Geng, T. He, R. Liu, S. Dalapati, K. T. Tan, Z. Li, S. Tao, Y. Gong, Q. Jiang and D. Jiang, *Chem. Rev.*, 2020, **120**, 8814–8933; (*c*) Q. Guan, L. L. Zhou and Y. B. Dong, *Chem. Soc. Rev.*, 2022, **51**, 6307–6416.

7 (*a*) B. Han, L. Zhang, L. Yunfei, B. Bin, E. Jie, L. Q. Zhang, Z. Xie, H. Wang and J. Jiang, *Adv. Funct. Mater.*, 2024, 2404289; (*b*) Q. Zhang, B. Han, Y. Jin, M. Li, E. Zhang and J. Jiang, *Chin. Chem. Lett.*, 2024, 110330; (*c*) X. Wang, M. Bahri, Z. Fu, M. A. Little, L. Liu, H. Niu, N. D. Browning, S. Y. Chong, L. Chen, J. W. Ward and A. I. Cooper, *J. Am. Chem. Soc.*, 2021, **143**, 15011–15016; (*d*) X. Wang, T. Fellowes, M. Bahri, H. Qu, B. Li, H. Niu, N. D. Browning, W. Zhang, J. W. Ward and A. I. Cooper, *J. Am. Chem. Soc.*, 2024, **146**, 14128–14135.

8 (*a*) P. M. Budd, S. M. Makhseed, B. S. Ghanem, K. J. Msayib, C. E. Tattershall and N. B. McKeown, *Mater. Today*, 2004, **7**, 40–46; (*b*) H. J. Mackintosh, P. M. Budd and N. B. McKeown, *J. Mater. Chem.*, 2008, **18**, 573–578.

9 R. Tamura, T. Kawata, Y. Hattori, N. Kobayashi and M. Kimura, *Macromolecules*, 2017, **50**, 7978–7983.

10 (*a*) Y.-K. Im, D.-G. Lee, H.-J. Noh, S.-Y. Yu, J. Mahmood, S. Lee and J.-B. Baek, *Angew. Chem., Int. Ed.*, 2022, **61**, e202203250; (*b*) Y. Wang, M. Wang, T. Chen, W. Yu, H. Liu, H. Cheng, W. Bi, M. Zhou, Y. Xie and C. Wu, *Angew. Chem., Int. Ed.*, 2023, **47**, e202308070.

11 S. Shimizu, A. Miura and N. Kobayashi, *CrystEngComm*, 2013, **15**, 3759–3762.

12 (*a*) O. Delgado-Friedrichs, M. O'Keeffe and O. M. Yaghi, *Acta Crystallogr., Sect. A: Found. Crystallogr.*, 2003, **59**, 515–525; (*b*) V. A. Blatov, L. Carlucci, G. Ciani and D. M. Proserpio, *CrystEngComm*, 2004, **6**, 377–395.

13 J. Y. Jaung, K. Fukunishi and M. Matsuoka, *J. Heterocycl. Chem.*, 1997, **34**, 653–657.